Rate of decay of turbulent kinetic energy in abruptly stabilized Ekman boundary layers

Stimit Shah and Elie Bou-Zeid

Phys. Rev. Fluids **4**, 074602 — Published 3 July 2019

DOI: 10.1103/PhysRevFluids.4.074602

On the rate of decay of turbulent kinetic energy in abruptly-stabilized Ekman boundary layers

Stimit Shah* and Elie Bou-Zeid†
Department of Civil and Environmental Engineering, Princeton University
(Dated: April 10, 2019)

Under statically-stable conditions in wall-bounded flows, turbulence is generated by shear and dissipated by buoyancy and viscosity. Most studies have focused on the steady-state balance of this budget, but the time-evolution of the turbulence when the stabilizing buoyancy flux is first imposed is as important in many geophysical applications. In this letter, we utilize a new paradigm on the critical role of shear production damping by buoyancy to develop a quantitative model for the rate of decay of turbulent kinetic energy (TKE), at early and intermediate times, after buoyancy is abruptly imposed on a steady neutrally-stratified Ekman boundary-layer flow. Scaling analyses and reduced models are developed to obtain an expression for this rate of decay, which is then validated using results from direct numerical simulation (DNS). We further show that the TKE production term persists as a parameter outside of the classic stability parameter term (the flux Richardson number) under unsteady conditions, and is therefore needed to describe the dynamics of evolving stable boundary layers. The long-time steady dissipation-production-buoyancy balance is also analyzed using the same modeling framework and confirms that the damping of shear TKE production by buoyancy is the main agent for the reduction in TKE, while the direct role of buoyancy destruction is secondary.

I. BACKGROUND AND MOTIVATION

Statically-stable turbulent flows continue to be a topic of broad interest due to their ubiquitous geophysical manifestations and the inherent complexity of their dynamics [1–6]. However, while most studies focus on statistically-stationary conditions, real-world applications often involve the onset of unsteady stable conditions in flows that are initially neutrally- or even unstably-stratified. One example is the stabilization of the atmospheric boundary layer during the evening transition, where the TKE and fluxes decrease rapidly with time [7]. Under such unsteady conditions, turbulence might not remain in quasi-equilibrium with the mean flow and the "memory" of the turbulence could have an influence on its evolution [8]. This, along with other characteristics of stable flows, could manifest as a failure of various turbulence closure schemes [4, 9], but currently our understanding of the unsteady evolution of wall-bounded turbulent flows subjected to a rapid onset of stabilizing conditions remains inadequate to address their implications. This challenge motivates the current study.

Of particular interest in such flows is the rate at which turbulence decays after the transition to the statically-stable conditions. Some previous studies have addressed this question [7, 10]. Flores and Riley [10] for example analyzed the rate of decay of vertical-velocity variance in a stable boundary layer with time, but only for early times after the onset of stability. Nadeau *et al.* [7] on the other hand developed models for this rate of decay that assume the turbulence production is completely shut off and TKE then decays due to viscous dissipation and buoyant destruction. However, previous studies have shown that the turbulent production does not go to zero despite its sharp drop. The dynamics of the turbulence decay are more strongly controlled by the decrease in production rather than by the buoyant dissipation [11, 12]. This decrease in production is triggered by the reduction in vertical variance and mixing length that buoyancy initiates, which then lead to reduced downward momentum transport, reduced surface friction, and then finally to reduced TKE production [12].

Here, we quantify the rate at which the reduction in TKE evolves at short and intermediate time scales, as well as the steady-state balance at long time scales. Using DNS data and theoretical arguments, we model the gradual drop in turbulence production and the time-evolution of buoyant and viscous dissipations. We also assess the effects of direct buoyancy destruction in comparison to the drop in shear TKE production to provide theoretical evidence that the latter is the main factor leading to lower TKE under stable conditions (compared to neutral flows).

II. NUMERICAL AND PHYSICAL PARAMETERS

Despite the fact that large eddy simulation (LES) has become the backbone of atmospheric modeling under neutral and statically unstable conditions [13], here we elect to use DNS for the study of stable flows. While this limits the Re of the simulated flow, turbulence under stable conditions can become spatially and temporally intermittent [14–17], with reduced characteristic eddy size [18] and a high degree of anisotropy [3, 19]. This challenges some of the underlying assumptions in LES and thus when the scientific questions being addressed require

* stimit@alumni.princeton.edu
† ebouzeid@princeton.edu

the analysis of higher-order turbulence statistics, DNS is preferred.

The incompressible form of the Navier-Stokes equations with the Boussinesq approximation, along with the thermal energy budget equation, are solved numerically. The flow is driven by a mean barotropic (constant in height) horizontal pressure gradient that is expressed as an equivalent geostrophic wind, and experiences a Coriolis force that causes non-zero mean cross-stream velocity. The rotation in the velocity field due to Coriolis force is useful to generate a flow that is more similar to real geophysical flows (albeit at a lower Re), but effectively the role of rotation in the turbulence dynamics of the problem at hand is secondary. The horizontal directions of the computational domain are treated as periodic, while the vertical boundary conditions are no-slip with impermeability at the bottom wall ($u = v = w = 0$) and a stress-free impermeable surface with zero heat flux at the top (similar to a half-channel simulation). A constant temperature θ_0, lower than the free stream temperature θ_∞ above the boundary layer, is imposed at the wall. Further details on the governing equations and the numerical methodology used for the DNS, along with code validation for the same simulation used here, can be found in Shah and Bou-Zeid [12].

The parameters of the simulations relevant for this study are listed in table I. The three primary non-dimensional inputs, defined such that they can be computed a priori without using the simulation outputs, are: (i) the Reynolds number $Re_f = GD/\nu = G/(\nu f/2)^{1/2}$ (G is magnitude of the geostrophic wind speed aligned in the streamwise direction, D the laminar Ekman boundary layer depth, ν the kinematic viscosity, and f the Coriolis parameter); (ii) the initial surface gradient Richardson number $Ri_{0,0} = g\Gamma_{0,0}D^2/\theta_\infty G^2$ (at $t = 0$ and $z = 0$, $g = 9.81 ms^{-2}$ is the gravitational acceleration and $\Gamma_{0,0}$ the initial dimensional temperature gradient near the surface); and (iii) the Prandtl number $Pr = \nu/\alpha = 0.7$ (α is the thermal diffusivity). The corresponding bulk parameters are: the effective Reynolds number $Re_{\delta_t} = G\delta_t/\nu$, where δ_t is the initial (neutral) turbulent Ekman-layer depth scale, and the bulk Richardson number $Ri_b = g\ \Delta\theta\ \delta_t/\theta_\infty G^2$ where $\Delta\theta = \theta_\infty - \theta_s$. We simulate a latitude of 90° resulting in a Coriolis parameter $f = 1.454 \times 10^{-4}\,\mathrm{rad\,s^{-1}}$. We also non-dimensionalize time either with the Coriolis frequency that represents the inertial time scale in the flow ($t_i = tf$), or with the turnover time of eddies of size equal to the Obukhov scale at $t = 0$ ($t_t = tu_{*,t=0}/L$). The relation between the two non-dimensional times is: $t_t = t_i(\delta_t/L)$, and the values of δ_t/L needed for conversion are reported in table I.

Simulations carried out for this study are at a Reynolds number Re_f of 600; the influence of variation in Re is therefore not evaluated (but the reader can refer to Shah and Bou-Zeid [12] where we report results at three Re_f values). The computational domain size is $L_x \times L_y \times L_z = 36D \times 36D \times 25D$, yielding an L_z about 1.5 times larger than the dynamically-simulated turbulent boundary layer depth ($1.5\delta_t$). While these domain sizes might be small for strongly stable cases where streaks or patches of laminar flow are seen, the DNS analysis carried out in this paper is limited to the time periods before the collapse and laminarization of the flow (which occurs for the high Ri_b cases at later times); turbulence levels are hence still significant and the turbulent field is continuous. Thus, the domain sizes are sufficient for the present analysis: for flows with continuous turbulence we have checked that these domain sizes give the same results as longer domain sizes (see Shah and Bou-Zeid [12]).

Re_f	$Ri_{0,0}$	u_*/U_g	δ_t/D	Re_{δ_t}	Re_τ	δ_t/L	Ri_b
600	0	0.0595	17.85	10,710	637.0	0.0	0
	0.001	0.0581	17.43	10,458	622.0	0.219	0.100
	0.002	0.0572	17.16	10,296	612.3	0.386	0.200
	0.005	0.0523	15.69	9,414	559.9	0.819	0.501
	0.010	0.0494	14.82	8,891	528.8	1.273	1.003

TABLE I. Simulations carried out for this study and the relevant parameters. Here $\delta_t/D = u_{*,t=0}/fD$, where δ_t is neutral turbulent Ekman-layer depth scale, $D = (2\nu/f)^{1/2}$ is the laminar Ekman layer depth, $u_{*,t=0}$ is the neutral friction velocity at time 0, $Re_{\delta_t} = G\delta_t/\nu$, $Re_\tau = u_*\delta_t/\nu$, Obukhov length $L = -u_*^3\theta_{ref}/\kappa g H_{k,s}$ where θ_{ref} is reference temperature, $H_{k,s} = -\alpha\ d\langle\theta\rangle/dz|_0$ is kinematic heat flux at the surface, and $Ri_b = g\ \Delta\theta\ \delta_t/\theta_\infty G^2$.

The notation used in this paper is as follows: $u_j = \langle u_j\rangle + u'_j = U_j + u'_j$, $p = \langle p\rangle + p'$, $\rho = \langle\rho\rangle + \rho'$ and $\theta = \langle\theta\rangle + \theta'$, where angle brackets $\langle\ \rangle$ or capital letters denote Reynolds averaging and the fluctuating component is denoted by primes ($'$). Subscripts x, y and z are used interchangeably with 1, 2 and 3, respectively denoting the streamwise (relative to geostrophic wind since due to Coriolis there is a cross-stream flow near the wall), cross-stream, and vertical directions in the domain. Unless stated otherwise, averaging has been carried out over xy-planes, which are the wall-parallel periodic homogeneous flow directions. Since we analyze unsteady flows, no time averaging is performed.

III. ANALYSIS AND RESULTS

In this section, we will first establish, from DNS data, the applicability of the Monin-Obukhov similarity theory under the simulated stable conditions in the following subsection (A) and the dissipation-production time lag (subsection B). Then we will model the TKE drop rate (subsection C) at short, intermediate and long time scales. In subsection D, we show that the drop in TKE production is significantly larger than the buoyant destruction. In subsection E we illustrate that the dynamics of evolving stable boundary layers cannot be reduced to a Richardson number similarity.

A. Flux-gradient relations in the stable ABL

The Monin-Obukov similarity theory [20] (MOST) postulates that the average non-dimensional wind speed and temperature gradients (which are denoted by ϕ_m and ϕ_h respectively) in non-neutral diabatic boundary-layer flows can be expressed in terms of height z normalized by the Obukhov length L. This theory is just a stability correction to the log-law that recovers the latter under neutral conditions (both requiring a relatively high Re). MOST relations have been initially determined empirically, with more recent theoretical derivations of their canonical functional forms [21, 22]. In stable boundary layers, wind speed ($M = \sqrt{\langle u\rangle^2 + \langle v\rangle^2}$) and temperature gradients are usually assumed linear in the stability parameter z/L for $0 \le z/L < 1$ (Brutsaert [23], Stull [24], Li, Katul, and Bou-Zeid [25]):

$$\phi_m\left(\frac{z}{L}\right) = \frac{\kappa z}{u_*}\frac{\partial M}{\partial z} = 1 + \beta_m \frac{z}{L}, \tag{1}$$

where β_m is an empirical constant. Notice that since our highest δ_t/L is 1.273 (table I), the inertial sublayer will always be in the linear range of ϕ_m. The stability parameter z/L gives a measure of the relative importance of buoyant destruction (or production) of TKE relative to production by shear (like a flux Richardson number). The Obukhov length scale L (see definition in table 1) indicates the height at which buoyancy destruction (or production) is on the same order as TKE production by shear. Under neutral conditions where the kinematic heat flux at the surface $H_{k,s} = -\alpha\, d\langle\theta\rangle/dz|_0 = 0$, $z/L = 0$ and the traditional log-law is recovered with a non-dimensional velocity gradient $\phi_m = 1$.

Figure 1 shows the velocity profiles on a log-linear scale and figure 2 shows the variation of non-dimensional velocity gradient with height for the neutral and the two weakly-stable simulations under statistically-steady conditions (that is, averaged in space and in time over several large-eddy turnover times after the flow equilibrates to the new stabilizing surface buoyancy flux). For the strongly-stable simulations, the mean flow undergoes an inertial oscillation (see illustration and modeling for example in Momen and Bou-Zeid [26]) that makes it difficult to obtain converged statistics through time-averaging to verify the applicability of MOST. For the illustrated cases, the mean velocity gradients follow MOST despite the moderate Reynolds numbers. The value of the empirical constant β_m is approximately 9, higher than what has been observed in other studies in the atmosphere at much higher Reynolds numbers (where $\beta_m \approx 5$ is reported [24, 27–29]). The Reynolds-number dependence of this constant has been theoretically explained by Chung and Matheou [30] by considering the u-w cospectra model for the inertial range [30–32] in a stable regime. The important take away point from this section on the mean velocity and velocity gradient is that an inertial (log for neutral) layer develops in the DNS despite the moderate Reynolds number, and MOST is thus an applicable stability correction for the gradients in that layer. This needs to be established to justify the relevance of the results to real high Reynold-number geophysical flows and since later we will invoke MOST in our scaling analysis of the TKE decay rate.

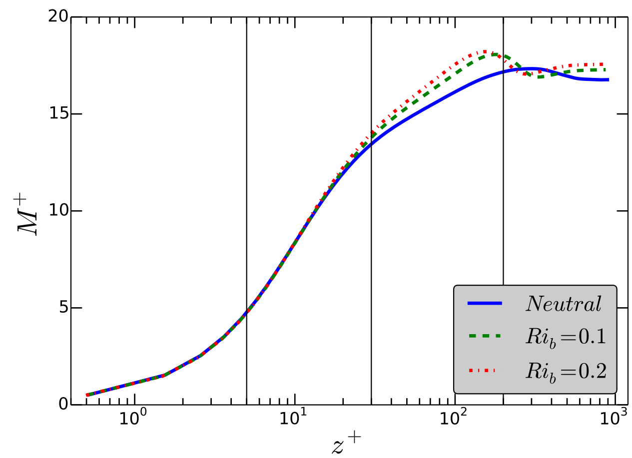

FIG. 1. Plot of mean velocity in inner coordinates, $M^+ = M/u_*$. Vertical black lines delimit the viscous sublayer ($z^+ \le 5$), buffer layer ($5 < z^+ \le 30$) and log-layer ($30 < z^+ \le 200$) for neutrally-stratified boundary layers.

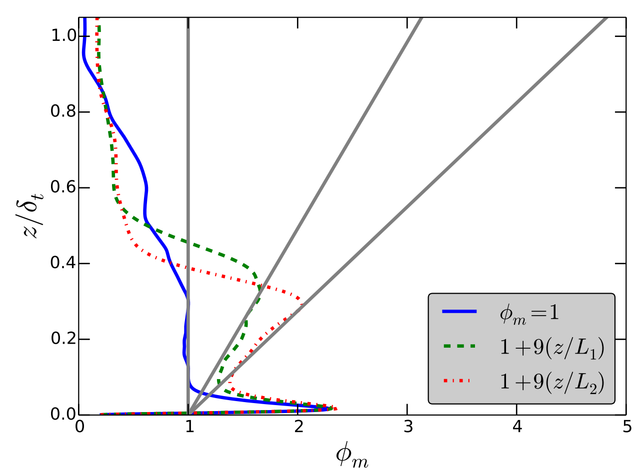

FIG. 2. Mean non-dimensional velocity gradient ϕ_m. Solid grey lines show the neutral boundary layer constant non-dimensional velocity gradient ($\phi_m = 1$), and the gradients predicted by MOST, $\phi_m = 1 + 9\frac{z}{L}$. The colored lines are the corresponding simulated profiles, where the solid blue line is for neutral conditions, dashed green line for $Ri_b = 0.100$ (with Obukhov length is L_1), and dot-dashed red line for $Ri_b = 0.200$ (with Obukhov length L_2).

B. Dissipation-production time lag

The correlation coefficient between TKE production and viscous dissipation, individually averaged over the whole domain, is shown in figure 3 as a function of a lag time τ introduced between the two time series. The plot indicates that the dissipation lags TKE production (since the correlation reaches a maximum at a time $\tau > 0$), which is expected. Moreover, a correlation coefficient of almost 1 is seen in the most stable case, and the peak correlation value increases monotonically with increasing stability (although the optimal time-lag does not vary monotonically, and given the limited statistical convergence due to the lack of time averaging, we are not certain the magnitude of the time lag itself is accurately captured). This indicates that dissipation lags production almost perfectly under stable conditions, meaning that the variations are strongly correlated if the appropriate lag is used. This might be a manifestation of the reduced role of transport in causing an imbalance between production and dissipation under higher stabilities. Hence, one can conclude that the lower total TKE in statically-stable flows is, as anticipated, not due to changes in viscous dissipation, which simply responds to production. The decrease in TKE as stability sets in must then be related with to buoyancy destruction or to a lower TKE production rate. The neutral case also displays a lag between dissipation and production, but the stronger TKE results in faster evolution and stronger transport of turbulence; therefore, the peak correlation is lower.

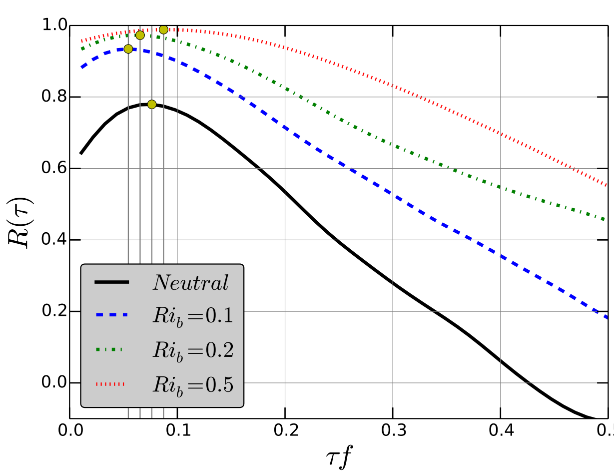

FIG. 3. Lagged correlation between TKE production and dissipation for neutral and stable cases $Ri_b = 0.1, 0.2, 0.5$, versus the non-dimensional time-lag τf. Vertical lines with filled circles depict the locations of maximum correlation.

C. Decay of vertical velocity variance and TKE

Figures 4 shows the decay with time of the vertical velocity variance ($\sigma_w^2 = \langle w'^2 \rangle$) at $z^+ \approx 50$ (inside the inertial layer), where the variance has been normalized by the squared friction velocity of the neutral flow at time $t = 0$. As noted by Flores and Riley [10], at early times, buoyancy flux is the primary term damping the vertical component of the TKE since the other terms respond more slowly to the onset of the stabilty. With a scaling analysis of the vertical velocity variance budget at short times, they were able to conclude that the time (t_{c1}) for its decay in the buffer layer ($z^+ = 15$) to its new stably-stratified equilibrium scales with $L/u_{*,t=0}$ (the scaling was found to depend on $h/u_{*,t=0}$ in the outer layer). We confirm (not shown) the same behavior in our simulations inside the buffer layer ($z^+ = 15$, where the TKE production is maximum), as well as at the interface between the buffer layer and the log-layer ($z^+ \approx 30$). Furthermore, the results in figure 4 indicate that the same scaling of the decay time of σ_w^2 with $L/u_{*,t=0}$ applies in the log-layer at $z^+ \approx 50$.

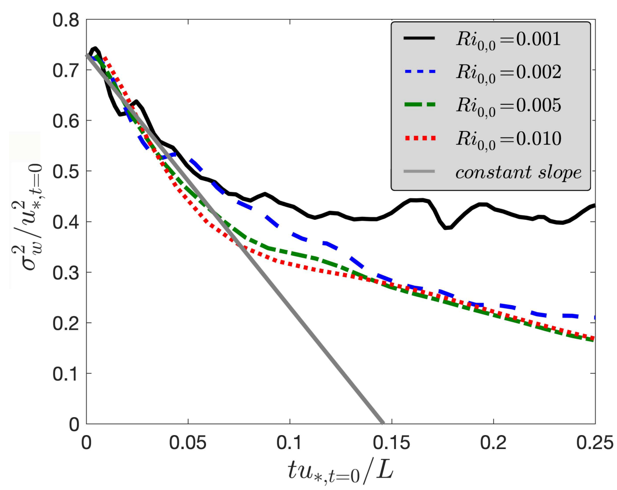

FIG. 4. Decay of the normalized vertical velocity variance with time normalized by $L/u_{*,t=0}$ at different stabilities at $z^+ \approx 50$. Note that $u_{*,t=0}$ is the same for all cases since it is the neutral friction velocity. Linear decay as predicted by Flores and Riley [10] is shown with solid grey line.

We now aim to extend the analysis and apply it to the full TKE budget equation. Due to anisotropy under stable conditions, the horizontal variances and the TKE ($q = \frac{1}{2}\langle u_i' u_i' \rangle$) might not scale similarly to the vertical variance and one could conceive of situations where the vertical variance is completely damped while two-dimensional turbulent motions persist in the horizontal directions. Moreover, the damping of the horizontal variances would not only be affected by buoyancy destruction (which directly acts on the vertical component), but also potentially by a drop in the shear production (which appears in the budgets of the horizontal variances), and the lagged drop in viscous dissipation. Despite these considerations, the drop in the TKE depicted in figure 5 (using the same normalization as the σ_w^2 plot in 4) suggests that its decay time also scales with $L/u_{*,t=0}$. However, the decay time of TKE is about one or two orders of magnitude larger than for the vertical component. In addition, the figure suggests that this linear decay extends till $tL/u_{*,t=0} \approx 2.5$ for all cases.

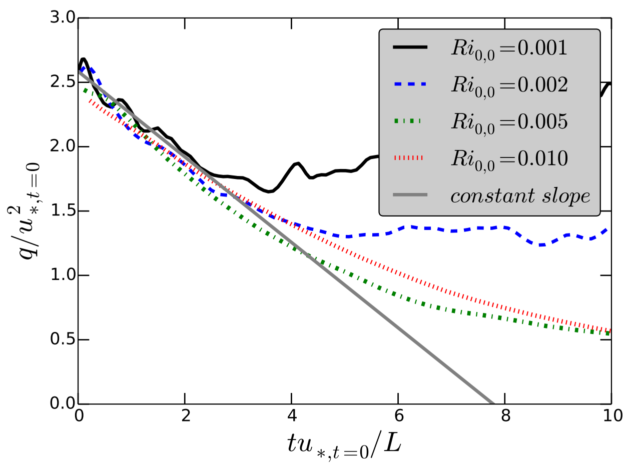

FIG. 5. Decay of normalized TKE ($q/u^2_{*,t=0}$) with time normalized by $L/u_{*,t=0}$ at different stabilities at $z^+ \approx 50$. Note that $u_{*,t=0}$ is the same for all cases since it is the neutral friction velocity. Linear decay rate is shown with grey solid line.

Another subtle difference to note at very early times ($tL/u_{*,t=0} < 0.2$) is that, while the vertical variance decays rapidly, the full TKE at that early point is less affected for the lowest stabilities. Separate plot of the horizontal components of the TKE (not shown) confirms that they do not start to decay until about $tL/u_{*,t=0} \approx 0.2$. This is not surprising since w is the component directly and most rapidly influenced by buoyancy and the onset of stability. The response of the horizontal components to buoyancy is indirect, first through pressure redistribution [33] and then through drop in production, and as such it is slower to develop. To analyze this drop in q and its scaling, we consider the full TKE budget. The transport terms will be neglected since under stable conditions they are even smaller than under neutral or convective conditions (in absolute and relative terms) [12]. These assumptions are comparable to the ones used to study the TKE drop in initially-convective boundary layers after the removal of the destabilizing surface buoyancy flux [34, 35]. Nieuwstadt and Brost [34] found that the TKE drops as $-tw_*/\delta_t$ if the heat flux is shut off suddenly (w_* being the convective velocity scale that is based on the surface buoyancy flux). While this is expectedly different from our scaling, both the δ_t/w_* in the convective case and the L/u_* in the stable case approximate the turnover time of the largest eddies in the flow that dominate the turbulence response.

The TKE budget equations under stable conditions is given by $\partial q/\partial t \approx P + B - \varepsilon$. We will consider that all the terms are averaged in space as a surrogate for Reynolds averaging. Here, P, B, and ϵ are the time-varying shear production, buoyant destruction and viscous dissipation terms, respectively. Substituting expressions for the dominant components of each of the above terms in the inertial layer, and then invoking Monin-Obukhov similarity to express them (lumping the production terms in the two horizontal directions) yields

$$\frac{\partial q}{\partial t} \approx -\langle u'w'\rangle\frac{\partial U}{\partial z} - \langle v'w'\rangle\frac{\partial V}{\partial z} + \frac{g}{\theta_{ref}}\langle w'\theta'\rangle - \varepsilon \quad (2)$$

$$\frac{\partial q}{\partial t} \approx u_*^2\frac{u_*}{\kappa z}\left(1+\beta\frac{z}{L}\right) - \frac{u_*^3}{\kappa L} - \varepsilon. \quad (3)$$

The buoyancy term is directly related to the vertical turbulent heat flux $H_k = \langle w'\theta'\rangle$, which is downward and negative in a stable boundary layer, making buoyancy a sink of TKE. In the equation above, we assumed that (i) the total stress is approximately constant all the way to the top of the inertial layer, (ii) the viscous fluxes in the inertial layer are negligible. These two assumptions together imply that the turbulent stress magnitude at $z^+ = 50$ is approximately the surface stress magnitude $u*^2$. The viscous flux contribution at the $Re_{\delta_t} \approx 10,000$ that we simulate and in the inertial layer we focus on is $< 5\%$ of the total Shah and Bou-Zeid [12] (also see figures 7.3 and 7.4 in Pope [36]). The last assumption (iii) is that the gradients follow their MOST function as the flow adapts to the new stability; but the value of β might be different from the equilibrium value and might change in time.

The dissipation term under stable conditions also follows Monin-Obukhov similarity and previous studies suggest various functions of its variation with z/L [37, 38]. Here we will adopt a simple linear form for consistency with the gradient function expression:

$$\epsilon = \frac{u_*^3}{\kappa z}\phi_\varepsilon = \frac{u_*^3}{\kappa z}\left(1+\beta_\varepsilon\frac{z}{L}\right). \quad (4)$$

With this expression for dissipation, Eq. 3 becomes

$$\frac{\partial q}{\partial t} \approx \frac{u_*^3}{\kappa L}(\beta - \beta_\varepsilon - 1). \quad (5)$$

Some studies suggest an additive constant different from 1 in Eq. 4 for ϕ_ε, thus indirectly encoding the neglected effect of transport [38]. For the present scaling analysis, and to remain consistent with the assumed production-dissipation equilibrium under neutral steady-state conditions (when $z/L = 0$ in the equation), it is clear from Eq. 5 that the two additive constants in the gradient and dissipation MOST functions should be set equal and we will adopt the value of 1 for both (though the present model can be modified by future users to account for transport or other effects). In the following sections, we will analyze the TKE trends indicated by the budget above, with needed modifications, for various time horizons.

1. Early times: the rise of buoyancy destruction

As argued by Flores and Riley [10], at (very) early times one would expect the onset of buoyancy flux to be the fastest response in the flow since it triggers the onset of other responses. This is also consistent with the setup of the simulations where we abruptly impose a drop in wall temperature at time 0. The initial flow is highly turbulent and the imposed cooling of the wall allows a strong heat flux to develop early on (heat flux time series from our simulations reveal a rapid rise until $tf \approx 0.1$). The buoyancy term will thus increase significantly in magnitude (from its zero neutral value), while the wall-shear, TKE shear production, and dissipation decrease only slightly from their near neutral values. If at early times one approximates that $u_* \approx u_{*,t=0}$ (the mean flow responds slowly and the pressure-Coriolis-friction force balance constrains the rate of drop in friction velocity), and given that at these times the observed decrease in TKE with time is linear, Eq. (5) becomes

$$\frac{\partial q}{\partial t} \approx \frac{q(t) - q(0)}{t} \approx \frac{u_{*,t=0}^3}{\kappa L}(\beta - \beta_\varepsilon - 1) \tag{6}$$

yielding

$$\frac{q(t)}{u_{*,t=0}^2} \approx \frac{q(0)}{u_{*,t=0}^2} + \frac{\beta - \beta_\varepsilon - 1}{\kappa} \; \frac{t u_{*,t=0}}{L}. \tag{7}$$

First, note that for $q(t)$ to be decreasing with time, it must be that $\beta - \beta_\varepsilon < 1$. In fact the slope of the grey linear fit in figure 5 is ≈ -0.33, from which one can infer that $\beta - \beta_\varepsilon = 0.867$. Since $\beta - \beta_\varepsilon > 0$, the TKE would have increased if the -1 term in the equation, corresponding to the buoyancy term, was not present. This implies that at these early time the buoyancy destruction is critical. Second, the linear decrease of the TKE with the non-dimensional time suggested by the equation indeed agrees with the scaling observed in Fig. 5 up till $tu_{*,t=0}/L \approx 2.5$. However, this early phase with neutral values of the friction velocity cannot in fact last that long. As illustrated in Fig. 4, the rapid initial onset of buoyancy damps the vertical variance rapidly until $tu_{*,t=0}/L \approx 0.2$ only. In addition, times series of heat flux (not shown) indicate that, after its initial rapid rise, the heat flux plateaus for the lowest stability and even decreases for the higher ones when $tf \geq 0.1$. One thus needs to investigate the mechanisms for the continued self-similar drop in TKE up to $tu_{*,t=0}/L \approx 2.5$ despite the much-earlier stabilization of the vertical component, as well as the scaling of this continued TKE drop.

2. Intermediate times: the fall of shear production

Buoyancy preferentially damps the largest turbulent structure [18, 39], and during the initial phase where it dominates, these large flux-carrying eddies are weakened. The downward momentum flux and the friction velocity are then reduced, the flow away from the wall accelerates, and the stress magnitude decreases at all heights. This damps shear generation significantly. As illustrated above, dissipation also decreases but with a time lag since the smallest scales that dissipate the TKE are not directly damped by buoyancy. Since production and dissipation drop, one needs to use the current values, with the current friction velocity, of these quantities in Eq. 5. An equation similar to Eq. 7 can be derived with the time-local friction velocity:

$$\frac{q(t)}{u_*^2} \approx \frac{q(0)}{u_*^2} + \frac{\beta - \beta_\varepsilon - 1}{\kappa} \; \frac{t u_*}{L}. \tag{8}$$

Eq. 8 suggests a linear decay with the time normalized by the local friction velocity. This is indeed confirmed by our DNS, but Fig. 5 also indicates a linear decrease with the time scaled by the initial friction velocity. Eq. 8 can in fact be recast as:

$$\frac{q(t)}{u_{*,0}^2} \approx \frac{q(0)}{u_{*,0}^2} + \frac{\beta - \beta_\varepsilon - 1}{\kappa} \; \frac{u_*^3}{u_{*,0}^3} \frac{t u_{*,0}}{L}. \tag{9}$$

Thus, the continued linear decrease in TKE with $tu_{*,t=0}/L$ observed in the figures necessitates a stabilization of the friction velocity with time during this intermediate period such that $u_*^3/u_{*,t=0}^3 \approx$ constant. Indeed analysis of the time evolution of the friction velocity (reported in Shah and Bou-Zeid [12]) confirms that it drops by 10 to 20% relative to the neutral value but stabilizes (or even recovers slightly) at $tf \geq 1$. This can be understood in the Ekman boundary layers since the driving pressure gradient is constant and the pressure force has to be balanced by wall friction and the Coriolis force. Therefore, wall friction remains on the same order as the neutral value even if the flow completely laminarizes, viscous stresses then having to sustain the downward momentum flux. The slope of the drop in TKE during these intermediate times however is reduced compared to the early times by a factor $u_*^3/u_{*^3_{t=0}}$. This period extends from $tu_{*,t=0}/L \approx 0.1$ up to $tu_{*,t=0}/L \approx 2.5$.

A major assumption in the scaling for these intermediate times that we made is that MOST-like scaling for production and dissipation still holds, despite the divergence of the trends of these TKE budget terms and of the friction velocity. An a priori justification for this assumption is that during this phase the turbulence maintains its neutral initial characteristics while it decays. An a posteriori support for its plausibility is the success of the scaling in matching the DNS results. However, the scaling can indeed be maintained even if the values of β and β_ε are different from their equilibrium or neutral values. This is why we refer to the models of production and dissipation as MOST-like. The model for buoyancy on the other hand is exact.

3. Later times: the return to equilibrium

At long times, the heat flux will start to decrease as the fluid near the surface cools down and the difference between the fluid and (constant) wall temperature decreases, causing the Obukhov length scale to increase. From Eq. 5, it can be noted that this will reduce the decay rate of the TKE, indeed as observed in Fig. 5. Eventually, a new equilibrium will be reached (though inertial oscillations can significantly delay its onset) where, if MOST holds, one should observe $\beta = \beta_\varepsilon + 1$ (or a similar form if the additive constants are not taken equal). In the high-*Re* ABL under steady conditions, the usual values found are $\beta_\varepsilon \approx 2.5$ and $\beta \approx 5$ [38]. In addition, as pointed out before, the additive constant in the dissipation is empirically found to be < 1, indicating that under neutral conditions production exceeds dissipation and transport must compensate for the difference in the inertial surface layer. These two observations then strongly indicate that transport must also play a role in the TKE budget of the inertial layer [40], violating a key assumption of MOST. This role will be important under steady conditions when the other terms are constant in time. Furthermore, if the imposed stability is high, the strongly-stable flow will also not obey MOST [3, 41–43]; however, here we presume the turbulence is always continuous and thus in the mildly stable regime.

Despite these observations, we note that Fig. 2 indicates that the steady state gradients can still be described using a form similar to MOST. The local shear that enters into the TKE production terms will not be equal to u_*^2, but will remain proportional to that surface stress. In addition, the buoyancy term as expressed in Eq. 3 is exact since it is just re-expressing the buoyancy flux. Therefore, it is reasonable to retain the models of the production and buoyancy used thus far. The dissipation term on the other hand will no longer follow the MOST relations; this has been verified using the current DNS data and suggested in other studies (see discussion and comparison in Hartogensis and De Bruin [38]). A modified model of the dissipation is thus needed. First, we re-write Eq. 3 without a specific dissipation expression as:

$$\frac{\partial q}{\partial t} \approx \frac{u_*^3}{\kappa z} + \frac{u_*^3}{\kappa L}(\beta - 1) - \varepsilon. \tag{10}$$

Since the equilibrium plateau reached by the TKE is a valuable parameter to know in stable flow, we consider the above equation when the new steady state is reached and $\partial q/\partial t = 0$. The dissipation at that point can be expressed as

$$\epsilon \approx \frac{u_*^3}{\kappa}\left(\frac{1-\beta}{L} - \frac{1}{z}\right). \tag{11}$$

In the above equation, since $\beta \approx 9 > 1$, dissipation ϵ is always negative as expected. One can also note that if $z \ll L$, the second term dominates the right hand side of Eq. 11 dominates and the dissipation is controlled by proximity to the wall (buoyancy is weak and viscous dissipation balances production as under neutral conditions). On the other hand, given that $\beta \approx 9$, it is sufficient for that $z \sim L$ for the first term in the parentheses to dominate. Stability then controls the rate of viscous dissipation (indirectly via how much is left for viscosity to dissipate after buoyant destruction) independently from z. This second limit is consistent with the so-called z-less scaling of the stable boundary layer [44].

Since the dissipation strongly depends on how much TKE is present in the domain, a commonly-used alternative to the MOST model for ε can be formulated as $\epsilon \approx -q^{3/2}/\Lambda$, where Λ is a length scale that includes any proportionality constant needed. A physically more transparent way of writing this model is $\epsilon \approx -q(q^{1/2}/\Lambda)$, where $q^{1/2}/\Lambda$ is an energy cascade inverse time scale associated with the turnover of the large large eddies that control the rate of energy production and cascade. Based on this model and Eq. 11, we can write:

$$\frac{-q^{3/2}}{\Lambda} \approx \frac{u_*^3}{\kappa}\left(\frac{1-\beta}{L} - \frac{1}{z}\right) \tag{12}$$

$$\frac{q}{u_*^2} \approx \left(\frac{\Lambda}{\kappa}\left(\frac{\beta-1}{L} + \frac{1}{z}\right)\right)^{2/3}. \tag{13}$$

Λ here is the characteristic large eddy scale that will be the smallest of L or z. Under weakly stable conditions when $z << L$ and $\Lambda \sim z$ one obtains:

$$\frac{q}{u_*^2} \approx \left(\frac{C_{\Lambda/z}}{\kappa}\right)^{2/3}, \tag{14}$$

where $C_{\Lambda/z}$ is as indicated in the subscript the ratio Λ/z assumed constant and ~ 1 for these conditions. However, under more stable conditions when $z \sim L$ (but the stability must remain mild for the MOST linear gradient functions to apply), $\Lambda \sim L$ and we obtain:

$$\frac{q}{u_*^2} \approx \left(C_{\Lambda/L}\frac{\beta-1}{\kappa}\right)^{2/3}. \tag{15}$$

$C_{\Lambda/L} \sim 1$ again is the constant (under these conditions) ratio Λ/L.

In both limits, $q \sim u_*^2$, but the ratio q/u_*^2 is much higher under the mildly stable conditions than under the weakly stable ones (assuming both constants are ~ 1). Since this ratio is the TKE normalized by the surface stress, higher values represent a decrease in the efficiency of downward momentum transfer under increasingly stable conditions. Furthermore, since β decreases as the Reynolds number increases as discussed before, lower *Re* flows also have a reduced momentum transport efficiency.

D. Roles of drop in shear production versus buoyancy in TKE decay

To quantify the relative contributions of buoyancy destruction and drop in shear production towards the

TKE reduction, we will focus on the buffer layer around $z^+ \approx 30$ where the TKE shear production is maximum. The gradients at these heights are not strongly affected by buoyancy as shown in Fig. 2, and the production thus scales with u_*^3/kz without a MOST correction. We can then express the drop in this peak production as

$$P - P_n = \frac{u_*^3}{\kappa z} - \frac{u_{*,0}^3}{\kappa z},$$

where P is shear production at any time under stable conditions and P_n its initial value under neutral conditions. This reduction in production can then be compared to direct buoyancy destruction $B = -u_*^3/(\kappa L)$ as:

$$\frac{P - P_n}{B} = \left(\frac{z}{L}\right)^{-1}\left(\frac{u_{*,0}^3}{u_*^3} - 1\right) \tag{16}$$

For the simulations conducted here, $u_{*,0}^3/u_*^3$ ranges from 1.3 to 1.95. This ratio alone suggests a drop in production that is 30 to 95 % larger than buoyant destruction. However, upon considering also z/L, this ratio becomes much higher. The lowest δ/L in our simulations is 0.219; therefore, in the regions of peak production where $z << \delta$, we have $z/L << 1$ yielding a ratio of $(P - P_n)/B >> 1$. This confirms that the effect of buoyancy destruction is confined to early times and to direct reduction in momentum transport efficiency, while the significant drop in TKE is mainly a result of the drop in TKE production. The drop in production is caused by a drop in downward transport of momentum and the reduction in wall stress due to the damping of vertical motions by buoyancy, as elucidated in Shah and Bou-Zeid [12]. This ratio $(P - P_n)/B$ however can be ~ 1 for $z/L >\approx 2$ (if the same drop in u_* is assumed for simplicity). This implies that the role of buoyancy via direct destruction increases also linearly (as observed in other studies [9, 18]) with increasing z/L, which is expected since $z/L \approx Ri_f = -B/P$.

E. Role of TKE production as a parameter

It has been briefly argued by Shah and Bou-Zeid [12] that a stability parameter based on the balance between TKE production by shear and direct destruction by buoyancy, like the flux Richardson number or the Monin-Obukhov stability parameter z/L, might not be sufficient for describing the dynamics of stable Ekman layers. That hypothesis is better explored through the analysis we present in this paper using the equation of the rate of decay. For example, consider the TKE budget equation for stable conditions normalized by TKE production; under a local equilibrium assumption (that still allows for unsteady means) such that all transport terms are ignored for simplicity

$$P^{-1}Dq/Dt \approx 1 + P^{-1}\epsilon - Ri_f. \tag{17}$$

As can be seen here, TKE production generally persists as a parameter outside of the stability parameter term (given by flux Richardson number).

When the tendency term is small and the flow is near steady-state conditions, a production-buoyancy-dissipation balance is established such that the budget reduces to $P^{-1}\epsilon = Ri_f - 1$, a form where the production/dissipation ratio is a linear function of Ri_f. Under such conditions, similarity theories based on Ri_f can be developed since changes in Ri_f encode changes in the viscous dissipation to production ratio. This also applies to the Monin-Obukhov similarity theory.

However, for unsteady flows where the tendency is significant, the non-dimensional rate of the TKE variation $P^{-1}Dq/Dt$ not only depends on Ri_f, but also on $P^{-1}\epsilon$, which here is a parameter that can be independent from Ri_f. Under such conditions, an Ri_f based similarity is only applicable if $P^{-1}\epsilon$ is a universal function of Ri_f. Given the lag between dissipation and production and the potential lag between buoyancy variation and subsequent impacts on the TKE budget, there is no physical reason to expect this condition to be satisfied (and in fact the empirical evidence from the DNS used here points to its failure). Under such conditions, the TKE production, viscous dissipation, and buoyant destruction become independent and Ri_f cannot encapsulate all the dynamics of the unsteady stable flow.

We here should note that this emergence of a second relevant dimensionless parameter to characterize the dynamics is not restricted to unsteady flows, but will also be observed when transport is important. Chamecki, Dias, and Freire [45] proposed a two-dimensional phase space approach to characterize the state of the turbulence under such conditions. Freire *et al.* [40] then showed that the second dimensionless parameter (in their work related to transport) explains the observation of Kolmogorov turbulence at higher Richardson numbers than expected.

IV. CONCLUSIONS

We combine DNS and reduced models to investigate the evolution of turbulent kinetic energy following the onset of a stabilizing buoyancy flux in an initially neutral turbulent flow. First we establish that the mean velocity and velocity gradient profiles follow MOST, even at the moderate simulated Reynolds numbers our DNS can reach. Then we illustrate the lagged dissipation response, relative to the more rapid response of the turbulence shear production, after the onset of stabilizing buoyancy. We use these observations to develop a model, based on the TKE budget equation, to predict the evolution of turbulence in the inertial layer at various time scales after stability is imposed.

At very early times, buoyancy rises while production and dissipation remain about constant. This damps the vertical variance but has little impact on the horizontal variance and the total TKE since the vertical component's contribution is the smallest. The damping of the larger scales by buoyancy sets the stage for the intermediate times dynamics where the the contribution of buoyancy reaches a plateau and is rapidly overtaken by the reduction in shear production, while dissipation lags. Despite the different physics, the DNS and the reduced model indicate that the TKE drop for both early and intermediate time scales is linear in $-tu_{*,t=0}/L$, though the slope of the linear reduction with this time scale is different during early and intermediate times. At long times, dissipation catches up and we are able to identify two limiting regimes, a weakly stable one ($z \ll L$), where the TKE to surface stress ratio is controlled by the distance to the wall, and a mildly stable one ($z \sim L$), where that ratio is solely determined by the Obukhov length independent of z. In either regimes, we note that both increasing stability and decreasing Reynolds number reduce the effectiveness of turbulence in generating downward momentum flux and wall drag, as indicated by the decreasing value of the TKE normalized by the squared friction velocity.

These insights are then used to support two key findings of this study: 1) The lower total TKE in statically stable flows, compared to an otherwise similar neutral flow, is mainly due to smaller TKE production rate and not because of buoyant destruction. We support this using a scaling analysis that illustrates that even at a $z/L \approx 1$, buoyancy destruction explains only about a third of the TKE reduction. 2) TKE production persists as a flow parameter independent of the classic stability parameter term (given by flux Richardson number) under unsteady conditions. Another dimensionless number, such as P/ε, is then needed to fully characterize the turbulence.

V. ACKNOWLEDGMENTS

This study was supported by the National Science Foundation's Division of Physical and Dynamics Meteorology under AGS-1026636 and by the Siebel Energy Grand Challenges Program at Princeton University. The authors would also like to acknowledge the critical role of the NCAR (Bluefire and Yellowstone) and PICSIE (Artemis and Della-3) computing resources.

[1] A. J. Thorpe and T. H. Guymer, "The nocturnal jet," Quarterly Journal of the Royal Meteorological Society **103**, 633–653 (1977).
[2] J. C. R. Hunt, J. C. Kaimal, and J. E. Gaynor, "Some observations of turbulence structure in stable layers," Quarterly Journal of the Royal Meteorological Society **111**, 793–815 (1985).
[3] L. Mahrt, "Stratified atmospheric boundary layers," Boundary-Layer Meteorology **90**, 375–396 (1999).
[4] H. J. S. Fernando and J. C. Weil, "Whither the Stable Boundary Layer?" Bulletin Of The American Meteorological Society **91**, 1475–1484 (2010).
[5] G. G. Katul, A. Porporato, S. Shah, and E. Bou-Zeid, "Two phenomenological constants explain similarity laws in stably stratified turbulence," Physical Review E **89**, 023007 (2014).
[6] O. Williams, T. Hohman, T. Van Buren, E. Bou-Zeid, and A. Smits, "The effect of stable thermal stratification on turbulent boundary layer statistics," Journal of Fluid Mechanics **812** (2017), 10.1017/jfm.2016.781.
[7] D. F. Nadeau, E. R. Pardyjak, C. W. Higgins, H. J. S. Fernando, and M. B. Parlange, "A Simple Model for the Afternoon and Early Evening Decay of Convective Turbulence Over Different Land Surfaces," Boundary-Layer Meteorology **141**, 301–324 (2011).
[8] M. Momen and E. Bou-Zeid, "Mean and turbulence dynamics in unsteady Ekman boundary layers," Journal of Fluid Mechanics (2017), 10.1017/jfm.2017.76.
[9] J. Huang, E. Bou-Zeid, and J.-C. Golaz, "Turbulence and Vertical Fluxes in the Stable Atmospheric Boundary Layer. Part II: A Novel Mixing-Length Model," Journal Of The Atmospheric Sciences **70**, 1528–1542 (2013).
[10] O. Flores and J. J. Riley, "Analysis of turbulence collapse in the stably stratified surface layer using direct numerical simulation," Boundary-Layer Meteorology **139**, 241–259 (2011).
[11] F. G. Jacobitz, S. Sarkar, and C. W. Van Atta, "Direct numerical simulations of the turbulence evolution in a uniformly sheared and stably stratified flow," *Journal of Fluid Mechanics*, Journal of Fluid Mechanics **342**, 231–261 (1997).
[12] S. K. Shah and E. Bou-Zeid, "Direct numerical simulations of turbulent ekman layers with increasing static stability: modifications to the bulk structure and second-order statistics," Journal of Fluid Mechanics **760**, 494–539 (2014).
[13] E. Bou-Zeid, "Challenging the large eddy simulation technique with advanced a posteriori tests," Journal Of Fluid Mechanics **764**, 1–4 (2015).
[14] R. L. Coulter, "A case study of turbulence in the stable nocturnal boundary layer," Boundary-Layer Meteorology **52**, 75–91 (1990).
[15] B. J. H. Van de Wiel, R. J. Ronda, A. F. Moene, H. A. R. De Bruin, and A. A. M. Holtslag, "Intermittent turbulence and oscillations in the stable boundary layer over land. part I: A bulk model," Journal of the Atmospheric Sciences **59**, 942–958 (2002).
[16] B. J. H. Van de Wiel, A. F. Moene, R. J. Ronda, H. A. R. De Bruin, and A. A. M. Holtslag, "Intermittent turbulence and oscillations in the stable boundary layer over land. part II: A system dynamics approach," *Journal of the Atmospheric Sciences*, Journal of the Atmospheric Sciences **59**, 2567–2581 (2002).
[17] C. Ansorge and J. P. Mellado, "Global intermittency and collapsing turbulence in the stratified planetary boundary layer," Boundary-Layer Meteorology **153**, 89–116 (2014).

[18] E. Bou-Zeid, C. Higgins, H. Huwald, C. Meneveau, and M. B. Parlange, "Field study of the dynamics and modelling of subgrid-scale turbulence in a stable atmospheric surface layer over a glacier," Journal Of Fluid Mechanics **665**, 480–515 (2010).

[19] Y. Ohya, D. E. Neff, and R. N. Meroney, "Turbulence structure in a stratified boundary layer under stable conditions," Boundary-Layer Meteorology **83**, 139–161 (1997).

[20] A. S. Monin and A. M. Obukhov, "Basic laws of turbulent mixing in the surface layer of the atmosphere, [From translation to English by John Miller, 1959]," Tr.Akad. Nauk SSSR Geophiz. Inst. **24**, 163–187 (1954).

[21] G. G. Katul, A. G. Konings, and A. Porporato, "Mean Velocity Profile in a Sheared and Thermally Stratified Atmospheric Boundary Layer," Physical Review Letters **107**, 268502 (2011).

[22] G. G. Katul, D. Li, M. Chamecki, and E. Bou-Zeid, "Mean scalar concentration profile in a sheared and thermally stratified atmospheric surface layer," Physical Review E **87**, 023004 (2013).

[23] W. Brutsaert, *Evaporation into the atmosphere: theory, history, and applications* (D. Riedel Publishing Company, 1982).

[24] R. B. Stull, *An introduction to boundary layer meteorology* (Kluwer, 1988) p. 670.

[25] D. Li, G. G. Katul, and E. Bou-Zeid, "Mean velocity and temperature profiles in a sheared diabatic turbulent boundary layer," Physics of Fluids **24**, 105105–16 (2012).

[26] M. Momen and E. Bou-Zeid, "Analytical Reduced Models for the Non-stationary Diabatic Atmospheric Boundary Layer," Boundary-Layer Meteorology **164** (2017), 10.1007/s10546-017-0247-0.

[27] E. K. Webb, "Profile relationships: The log-linear range, and extension to strong stability," Quarterly Journal of the Royal Meteorological Society **96**, 67–90 (1970).

[28] A. J. Dyer, "A review of flux-profile relationships," Boundary-Layer Meteorology **7**, 363–372 (1974).

[29] J. Kondo, O. Kanechika, and N. Yasuda, "Heat and momentum transfers under strong stability in the atmospheric surface layer." Journal of Atmospheric Sciences **35**, 1012–1021 (1978).

[30] D. Chung and G. Matheou, "Direct numerical simulation of stationary homogeneous stratified sheared turbulence," Journal of Fluid Mechanics **696**, 434–467 (2012).

[31] J. L. Lumley, "Similarity and the turbulent energy spectrum," Physics of Fluids **10**, 855–858 (1967).

[32] J. C. Wyngaard and O. R. Coté, "Cospectral similarity in the atmospheric surface layer," Quarterly Journal of the Royal Meteorological Society **98**, 590–603 (1972).

[33] E. Bou-Zeid, X. Gao, C. Ansorge, and G. G. Katul, "On the role of return to isotropy in wall-bounded turbulent flows with buoyancy," Journal of Fluid Mechanics **856**, 61–78 (2018).

[34] F. T. M. Nieuwstadt and R. A. Brost, "The Decay of Convective Turbulence," Journal of the Atmospheric Sciences **43**, 532–546 (1986).

[35] Z. Sorbjan, "Decay of convective turbulence revisited," Boundary-Layer Meteorology **82**, 503–517 (1997).

[36] S. B. Pope, *Turbulent flows* (Cambridge University Press, Cambridge, 2000) p. 806.

[37] M. Pahlow, M. B. Parlange, and F. Porté-Agel, "On Monin-Obukhov similarity in the stable atmospheric boundary layer," Boundary-Layer Meteorology **99**, 225–248 (2001).

[38] O. K. Hartogensis and H. A. R. De Bruin, "Monin-Obukhov similarity functions of the structure parameter of temperature and turbulent kinetic energy dissipation rate in the stable boundary layer," Boundary-Layer Meteorology (2005), 10.1007/s10546-004-2817-1.

[39] F. Dalaudier and C. Sidi, "Some characteristics of the turbulent buoyancy subrange," Advances in Space Research (1990), 10.1016/0273-1177(90)90005-K.

[40] L. S. Freire, M. Chamecki, E. BouZeid, and N. L. Dias, "Critical flux Richardson number for Kolmogorov turbulence enabled by TKE transport," Quarterly Journal of the Royal Meteorological Society , qj.3511 (2019).

[41] S. S. Zilitinkevich, T. Elperin, N. Kleeorin, and I. Rogachevskii, "Energy- and flux-budget (EFB) turbulence closure model for stably stratified flows. Part I: Steady-state, homogeneous regimes Original Paper," Atmospheric Boundary Layers: Nature, Theory and Applications to Environmental Modelling and Security , 11–35 (2007).

[42] G. G. Katul, A. Porporato, S. Shah, and E. Bou-Zeid, "Two phenomenological constants explain similarity laws in stably stratified turbulence," Physical Review E **89**, 023007 (2014).

[43] D. Li, G. G. Katul, and S. S. Zilitinkevich, "Closure schemes for stably stratified atmospheric flows without turbulence cutoff," Journal of the Atmospheric Sciences **73**, 4817–4832 (2016).

[44] J. Wyngaard, "On surface layer turbulence." in *Workshop on Micrometeorology* (American Meteorological Society, 1973) pp. 109–149.

[45] M. Chamecki, N. L. Dias, and L. S. Freire, "A TKE-Based Framework for Studying Disturbed Atmospheric Surface Layer Flows and Application to Vertical Velocity Variance Over Canopies," Geophysical Research Letters (2018), 10.1029/2018GL077853.

[46] C. J. Nappo, "Sporadic breakdowns of stability in the pbl over simple and complex terrain," Boundary-Layer Meteorology **54**, 69–87 (1991).

[47] P. G. Duynkerke, "Observation of a quasi-periodic oscillation due to gravity waves in a shallow radiation fog," Quarterly Journal of the Royal Meteorological Society **117**, 1207–1224 (1991).

[48] J. C. Barnard, *Intermittent turbulence in the very stable Ekman layer*, Ph.D. thesis, University of Washington (2000).